the STAX proposal

Paolo SPAGNOLO
INFN - Pisa

Phys. Dark Univ. **12**, 37 (2016)

Physics of the Dark Universe 12 (2016) 37–44

Contents lists available at ScienceDirect

Physics of the Dark Universe

journal homepage: www.elsevier.com/locate/dark

Axion-like particle searches with sub-THz photons

L.M. Capparelli [a], G. Cavoto [b], J. Ferretti [c], F. Giazotto [d], A.D. Polosa [c,e,*], P. Spagnolo [f]

[a] Department of Physics and Astronomy, University of California Los Angeles, 475 Portola Plaza, Los Angeles, CA 90095, USA
[b] INFN Sezione di Roma, P.le Aldo Moro 5, I-00185 Roma, Italy
[c] Dipartimento di Fisica and INFN, 'Sapienza' Università di Roma, P.le Aldo Moro 5, I-00185 Roma, Italy
[d] NEST, Istituto Nanoscienze-CNR and Scuola Normale Superiore, I-56127 Pisa, Italy
[e] CERN-TH, CH-1211 Geneva 23, Switzerland
[f] INFN Sezione di Pisa, Largo Bruno Pontecorvo, 3, 56127 Pisa, Italy

A R T I C L E I N F O

Article history:
Received 23 October 2015
Received in revised form
28 January 2016
Accepted 29 January 2016

Keywords:
Axion-like particles
Dark-matter constituents
Paraphotons
Chameleons
Light-Shining-through-Wall experiments

A B S T R A C T

We propose a variation, based on very low energy and extremely intense photon sources, on the well established technique of Light-Shining-through-Wall (LSW) experiments for axion-like particle searches. With radiation sources at 30 GHz, we compute that present laboratory exclusion limits on axion-like particles might be improved by at least four orders of magnitude, for masses $m_a \lesssim 0.01$ meV. This could motivate research and development programs on dedicated single-photon sub-THz detectors.

Presented at ICHEP16

Axions Experiments

3 classes of experiments: Haloscopic, Helioscopic, Laboratory (LSW)

Axion, like neutral pion couples to two photons via Primakoff effect)
Detected in a magnetic field H

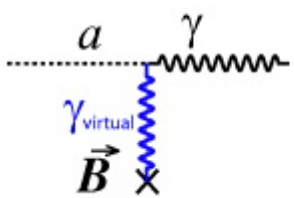

$m_a < 3x10^{-3}$ eV from SN1987

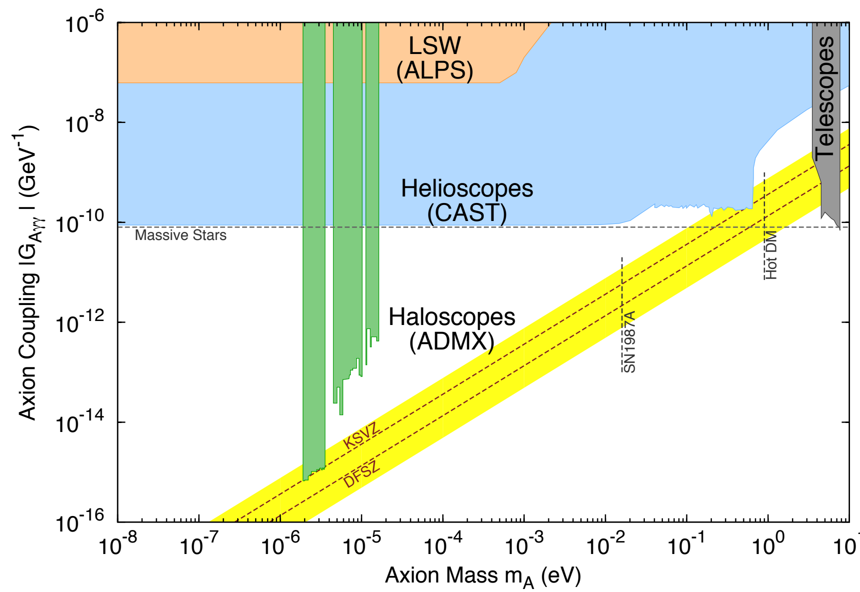

Yellow band represent theoretical predictions from DFSZ and KSVZ axion models

Haloscopic: cavity like ADMX (Livermore)
Are the only experiments hitting the Peccei-Quin region

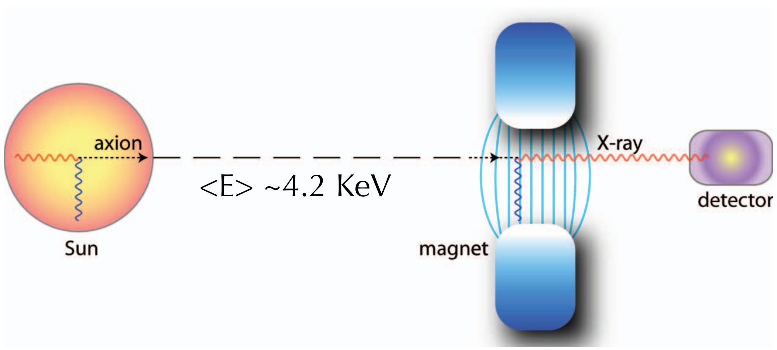

Helioscopic: depend on stellar models
CAST (best limit at the moment) and
IAXO (next CERN exp.) use LHC dipoles

Light Shining through a Wall Experiments

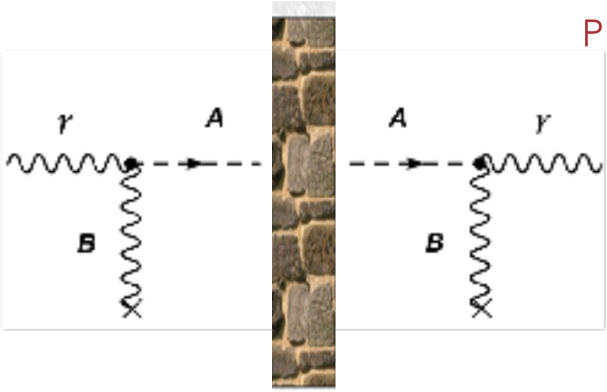

P. Sikivie, Phys. Rev. Lett. **51**, 1415 (1983)

LAB experiment
Laser Source
Higher Luminosity

Double process
Rate ~ G^4

$$\dot{N}_{\text{evts}} \propto \dot{N}_\gamma \, P_{\gamma\to a} \times P_{a\to\gamma} \sim \dot{N}_\gamma \, G^4 H^4 L^4$$

Sensitivity on G linear with L and H, quartic root of luminosity (not depending on E_γ)

The STAX key points are:

- High Luminosity (gyrotrons in the SubTHz region)
- intense H ~ 15 Tesla with L ~ 50 cm dipole
- Sub-THz single photon detector using TES

Optimal Working Point ~ 30 GHz

Light Shining through a Wall Experiments: ALPS

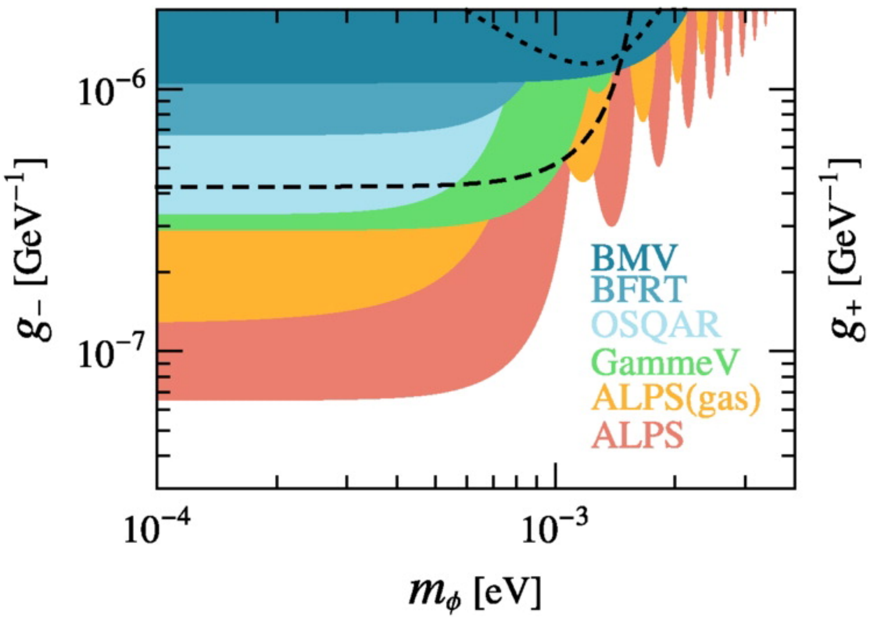

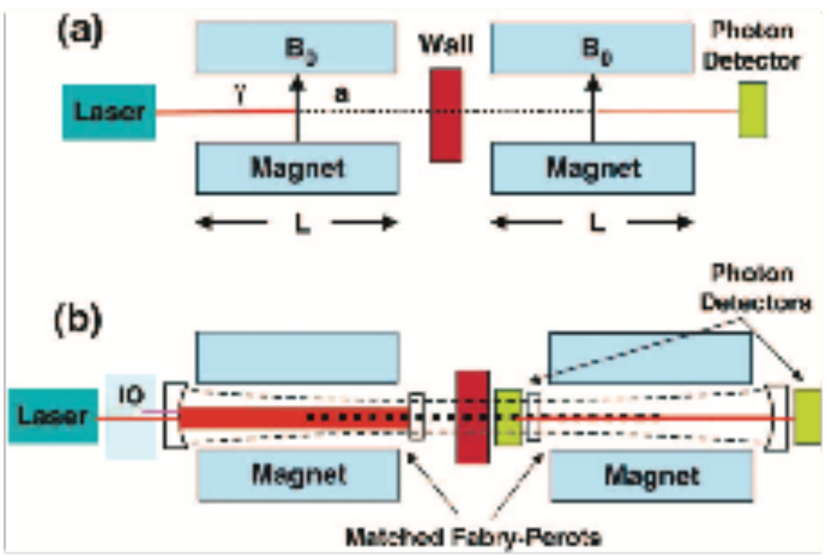

Ex: ALPS Desy use the Hera dipoles
N~ 10^{19} photons/s

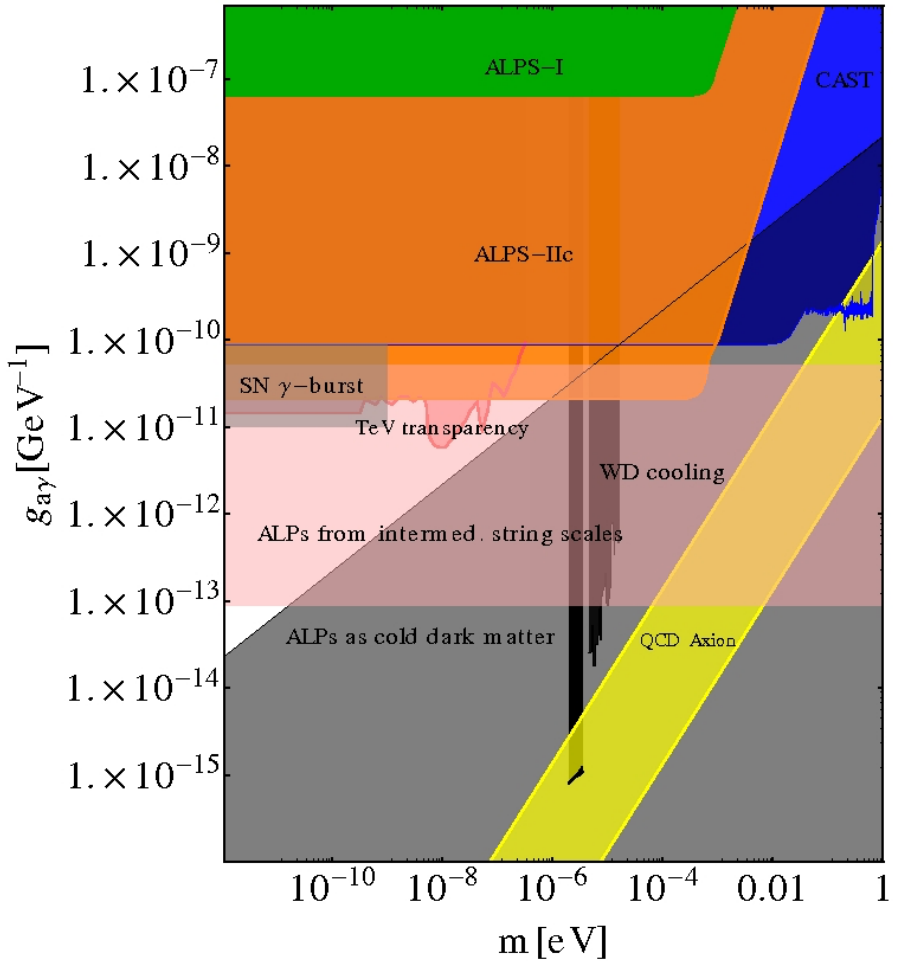

High Luminosity Photon Sources

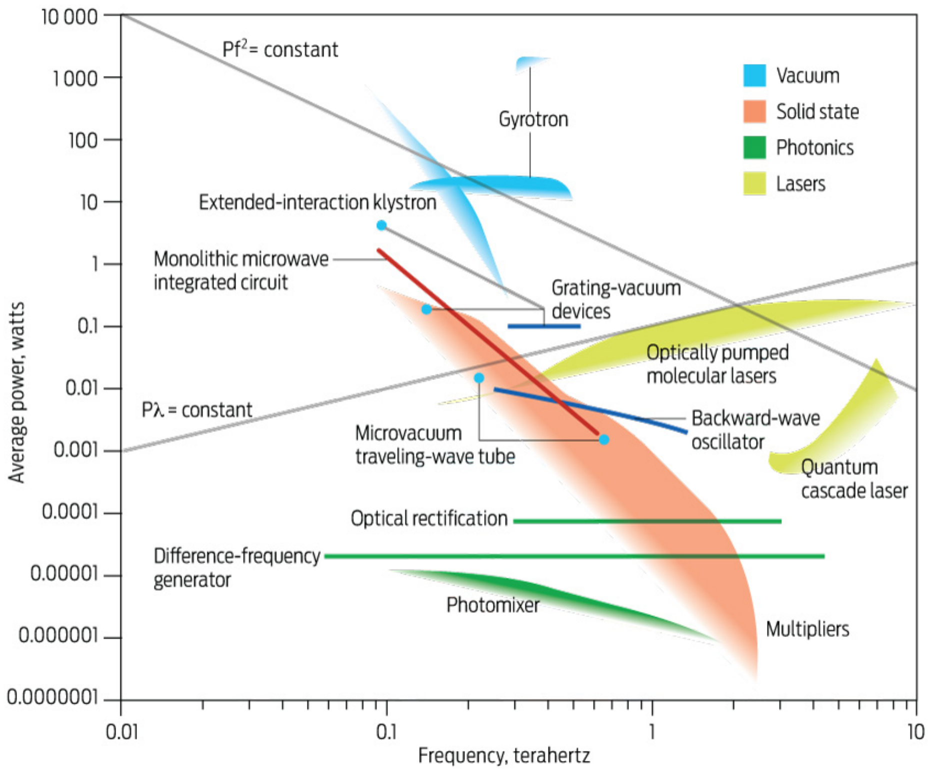

photon-axion conversion probability depends on luminosity, not energy
$\Rightarrow$ sub-THz

Reference:
30 GHz ~ 120 μeV ~ 1 cm
Micro-waves domain

- Klystrons and gyrotrons sources in the 30-100 GHz range.
- Power exceeding 1 MW in this frequency range
- Luminosity up to 10^{28}-10^{29} γ/s in CW
- Lasers commonly used in LSW experiments ~ 10^{19} γ/s

Gyrotrons

$P(\mathrm{MW}) \times \nu^2(\mathrm{GHz}^2) = \mathrm{const.}$

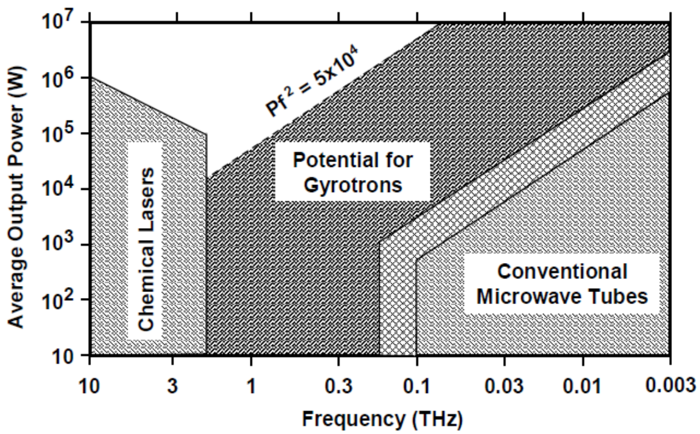

The operating region of gyrotrons

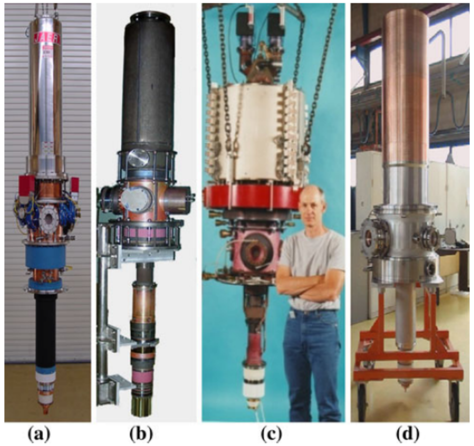

Fig. 2 Typical high power gyrotrons **a** JAERI/TOSHIBA 0.82 MW, 170 GHz, **b** GYCOM 1 MW, 170 GHz, **c** CPI 0.9 MW, 140 GHz, **d** TED 0.9 MW, 140 GHz

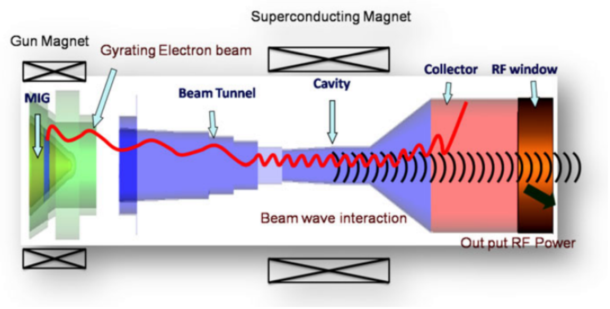

Now beyond 1 MW power

High-Power Cyclotron Autoresonance Maser (CARM)
Up to 10-15 MW with 10-50 GHz

STAX Experiment

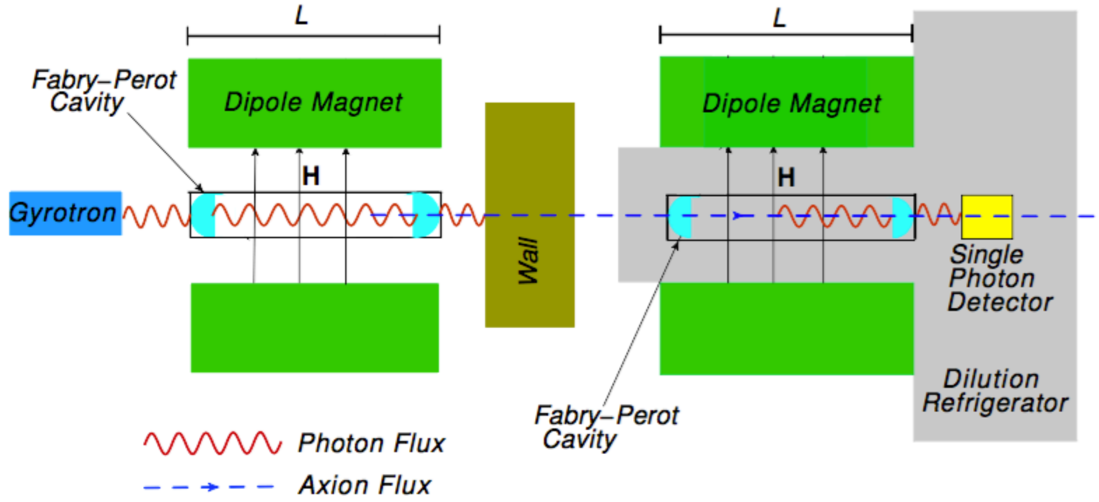

- Magnetic field: H = 15 T, L = 0.5 m
- Source: gyrotron; $P \approx$ 100 kW, $\Phi_\gamma = 10^{27}$ s^{-1}, ε_γ = 120 μeV ($\nu \approx$ 30 GHz)
- Fabry-Perot cavity: finesse $Q \approx 10^4$

- Sub-THz single-photon detection based on TES technology, $\eta \approx 1$
- Possible second FP cavity behind the wall to enhance axion-photon conversion rate

P. Sikivie, D.B. Tanner and K. Van Bibber, Phys. Rev. Lett. 98, 172002 (2007)

STAX detector

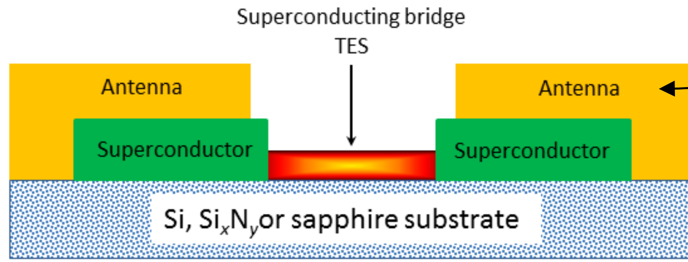

- Sub-THz single photon detector
- Transition Edge Sensor TES: ultra-low critical temperature superconductor bridge between two superconducting electrodes. TES coupled to a log periodic antenna.
- TES operates within its superconducting transition. DC bias voltage applied. When TES absorbs an incoming photon, it heats up above critical temperature Tc. Change of resistance and current flowing in the circuit, measured by a SQUID
- Material: choice of a Superconductor with low critical temperature ($T_c \approx 20$ mK) to have a good energy resolution α-W or bilayer Ti-Au or Ti-Cu
- TES bridge Ti-Cu (gap ~20 μeV), superconducting electrodes Nb (gap ~ 1 meV)
- Very high efficiency
- Ultra low background/dark count

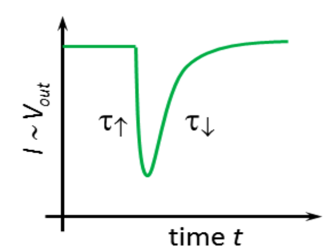

STAX detector

- Tailoring TES active volume to reduce thermal capacitance **($V \sim 10^{-3}$-10^{-4} μm^3)**

$$\sigma_E \approx 0.3\sqrt{k_B T_c^2 C_e}$$

$C = \gamma V T$ $V \sim 300 \times 40 \times 20$ nm ^{3}

- low-noise SQUID readout electronics optimization (operating at 80 mK)
- Sensitivity $\delta T = \delta E / C_e$ thermalization $T(t) = \exp(-t/\tau)$ $\tau = C_e / G$

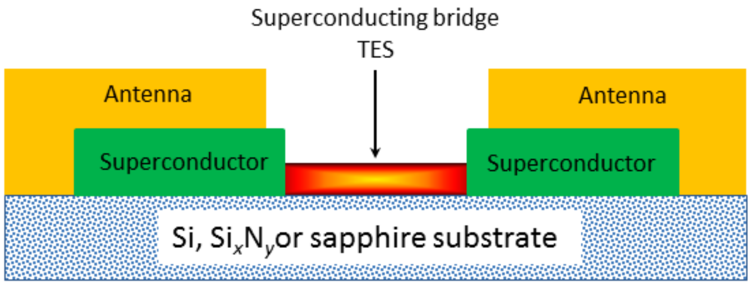

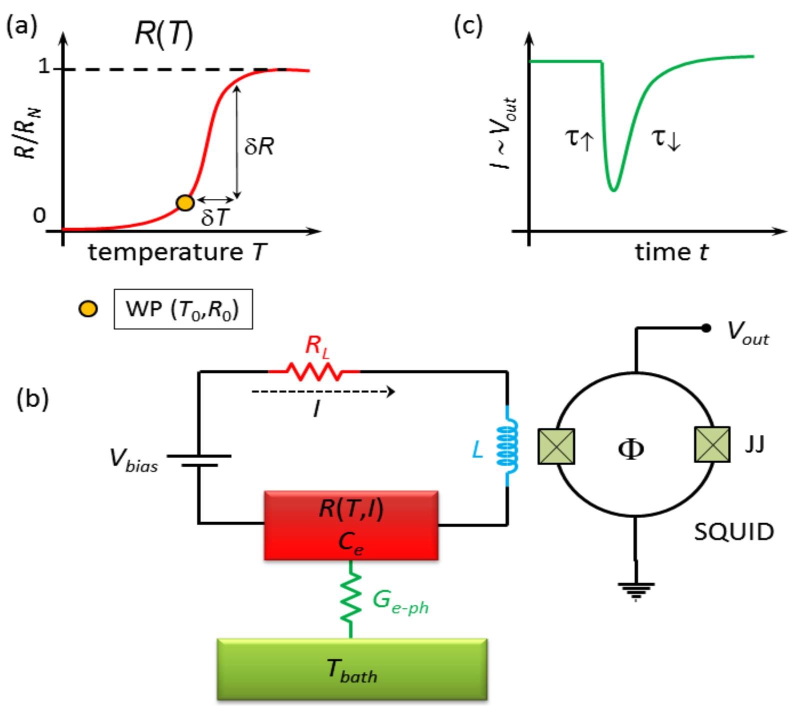

Noise

- Dark count rate (phonon noise) < 6×10^{-10} s^{-1}
- Black Body: at 10mK peaked around 0.6 GHz with a negligible rate of 10^{-30} m^{-2} s^{-1} photons irradiated
- Cosmic bkg: 1μ/cm^{-2}/min with 10 eV released in 10nm of material saturates the TES, bkg. under control translated in a negligible dead time of the TES ~ 0.1%

$$N_d = \frac{\beta_{eff}}{\sqrt{2\pi}} \int_{E_T/\sigma_E}^{\infty} exp(-x^2/2)\,\mathrm{d}x.$$

where $\beta_{eff} = 1/\tau_{eff}$ is the effective detection bandwidth, and E_T is the discrimination threshold energy.

$$\eta = \frac{1}{\sqrt{2\pi}} \int_{(E_T-h\nu)/\sigma_E}^{\infty} exp(-x^2/2)\,\mathrm{d}x.$$

Scheme of the temperatures in the experimental dilution cryostat set-up

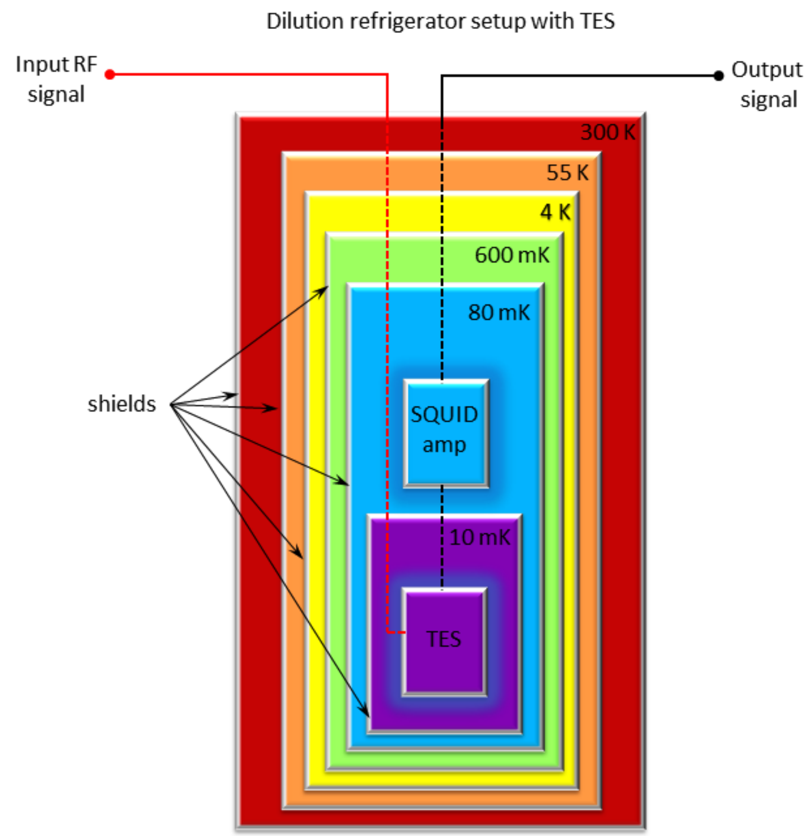

Figure 8 *Scheme of the experimental setup of the TES based on a dilution refrigerator. The cryostat metallic shields reside at different temperatures from 300 K to below ~ 10 mK. The enclosure containing the TES element is at the fridge base temperature whereas the readout SQUID amplifier is kept at 80 mK to improve its noise performance. Input microwave radiation is fed into the fridge, and thereby into the TES detector, via coaxial cables while the low-frequency output signal coming from the SQUID is read via conventional DC lines.*

$$P_{\gamma \leftrightarrows a} = g^2 H^2 \frac{\sin^2\left(\frac{q_x L_x}{2}\right)}{q_x^2}$$

$$q_x = \frac{m_a^2}{2\mathcal{E}_\gamma}$$

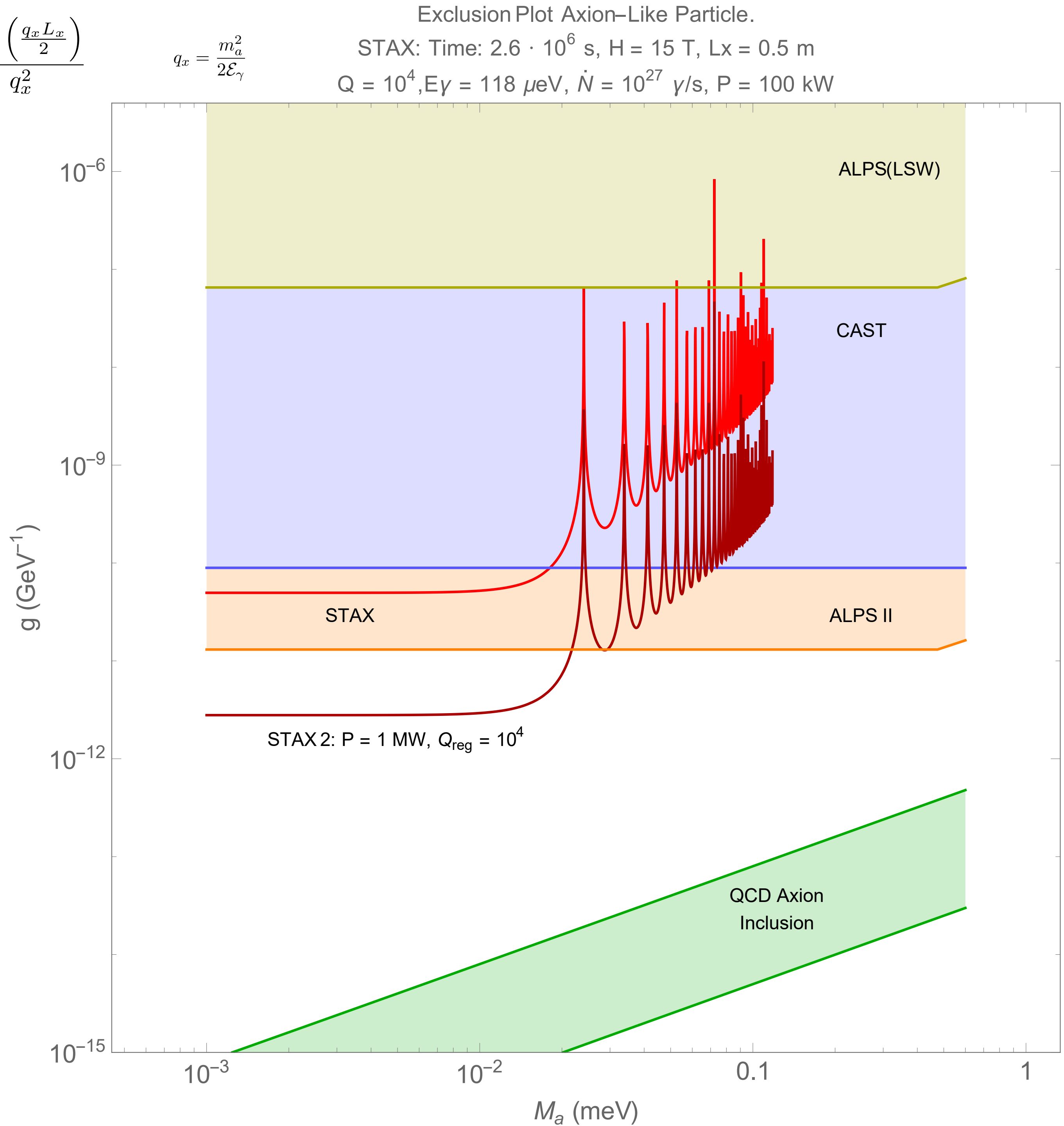

$2\text{x}10^{-11}$

$1.2\text{x}10^{-12}$

Parameter	ALPS	STAX	g_{ALPS} / g_{STAX}	STAX II	g_{ALPS} / g_{STAXII}
Laser Power	0.8 W	100 kW	18.8	1 MW	188
Photon Energy	2.327 eV	124 µeV	11.7	124 µeV	11.7
Cavity Q-factor	55.0	10^4	3.7	10^8	37
$H * L_x$	22 T m	7.5 T m	0.3	7.5 T m	0.3
Detection Efficiency	0.9	1.0	1.0	1.0	1.0
Detector Noise	$1.8\ 10^{-3}\ sec^{-1}$	$10^{-9}\ sec^{-1}$	34.0	$10^{-9}\ sec^{-1}$	34
Combined Improvement			~ 10^4		~ $8x10^5$

Alternative choices to boost the experiment

- Work with a new concept Fabry Perot to enhance the finesse Q
- An upgrade in Q translates into the need of a lower power of the source P/Q^2

$$\dot{N}_{evts} \propto \dot{N}_\gamma \, P_{\gamma \to a} \times P_{a \to \gamma} \times Q^2$$

- Fabry Perot with Q exceeding 10^{10} have been recently developed with superconducting cavities or *wispering galleries resonator*

- Material choice need to be shaped to work in this particular environment
  - Low temp
  - High B field
- High Q and lower P can drive the use of other (more refined and easier to handle) photon sources than gyrotrons (klystrons?)
- or also to a lighter B fiels (split coil vs solenoid?)

- **Cu/Al** and **Cu/Ti** bilayers designed as **5 μm X 200 nm strip** of different total thickness and thickness ratio

- Fabrication via e-beam lithography + e-beam evaporation

- 4-wires measurements of the resistance using a lock-in circuit

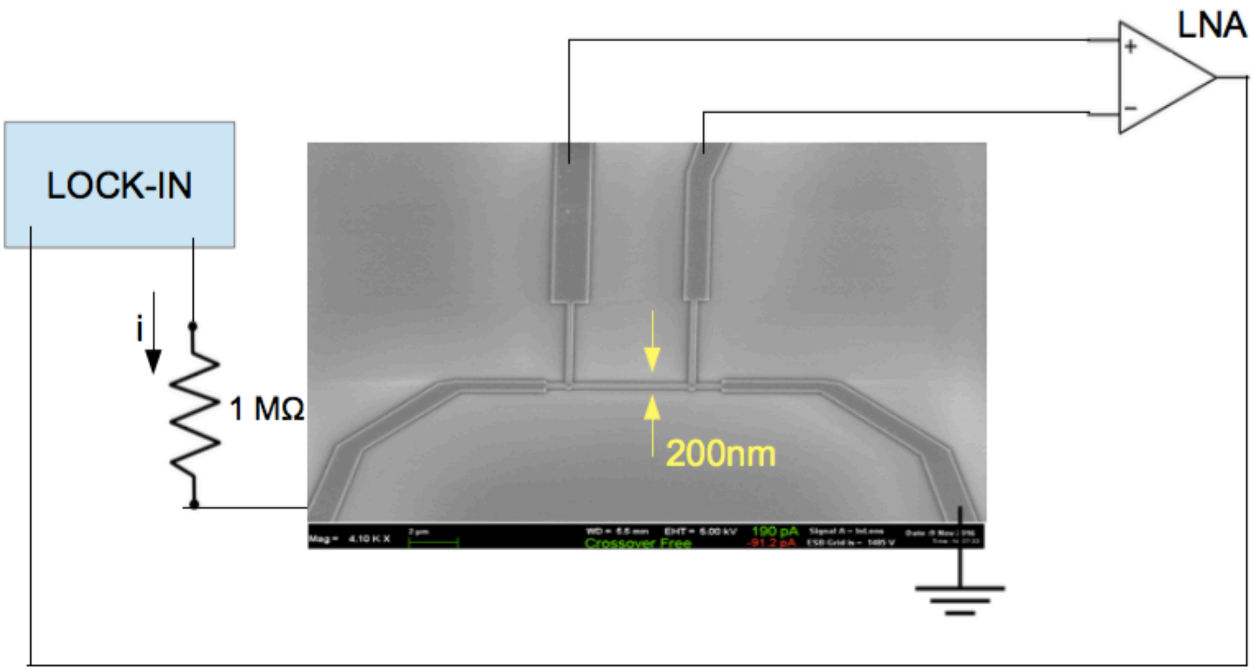

Tc of Cu/Al bilayers

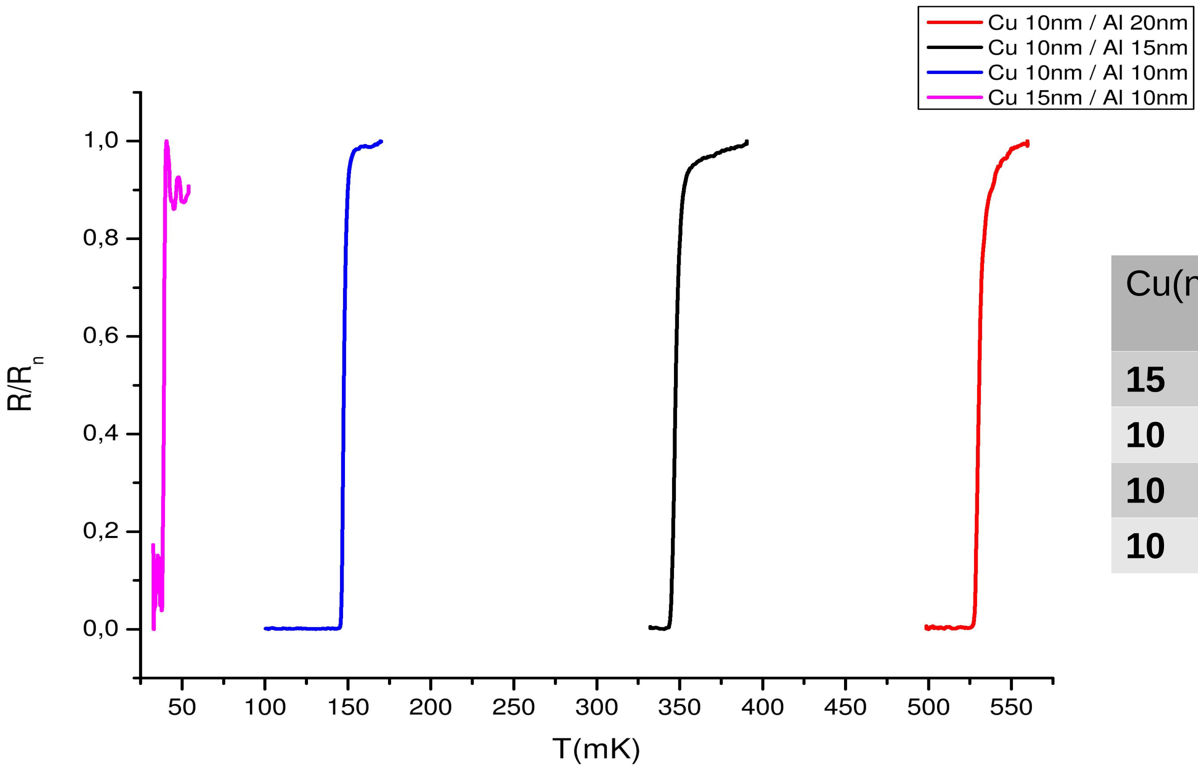

alpha=MAX(T/R dR/dT)

Cu(nm)	Al(nm)	Tc (mK)	Rn (ohm)	alpha
15	**10**	40	70	100
10	**10**	147	165	420
10	**15**	347	115	500
10	**20**	530	75	900

tional Enterprise for nanoScience and nanoTechnology

NEST

Tc of Cu/Al bilayers (1)

all transitions are measured with a lock-in circuit with input current i = 6nA, except for Cu15Al10 (i=0.1nA)

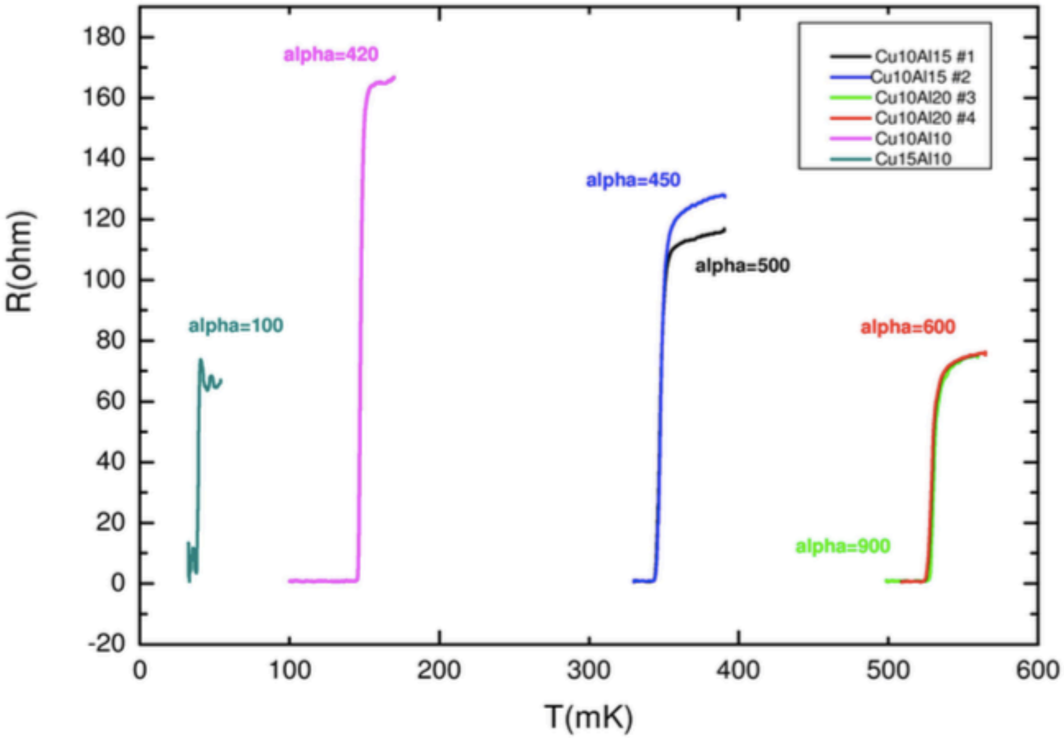

Data analysis: extraction of alpha=T/R * dR/dT

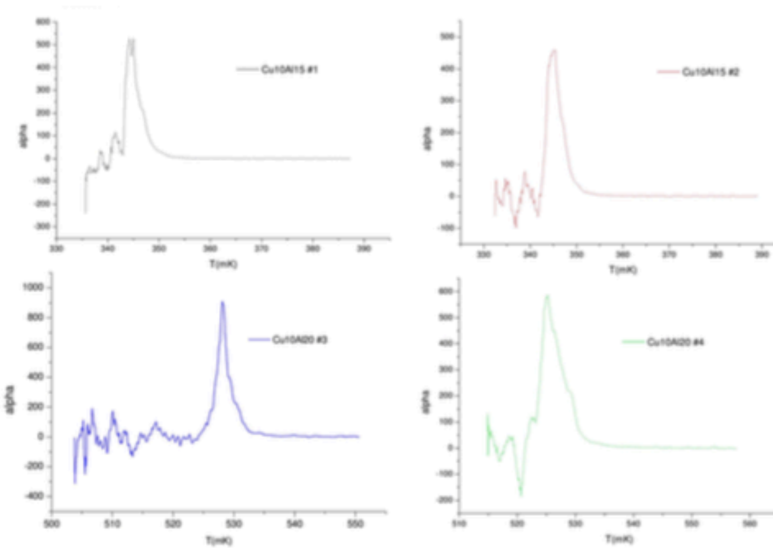

In the plot are reported the thicknesses and the max value of alpha

National Enterprise for nanoScience and nanoTechnology

NEST

Next Steps…

- Cu/Ti up down to Tc ~ 20mK
- Coupling with a SQUID read-out
- Test with a 30 GHz photon source
- R&D of the Fabry Perot
- Design of the log periodic antenna
- Magnet design

CONCLUSIONS

- A new optimized version of the LSW experiments is proposed
- The ambitious goal is to push limit on the photon-axion coupling G beyond stellar experiments (CAST) exclusion
- Development of Fabry-Perot and TES detectors could lead to a new generation of experiments in the field
- Important R&D need to be addressed to the scope

Nanotech detector could drive Particle Physics of Light Dark Matter

BACK UP SLIDES

BACK-UP

- Wavelength associated to virtual axion $\lambda = 1/p_x \approx L_x$
  Uncertainty principle: $\Delta x \approx L_x \rightarrow \Delta p \geq 1/L_x$
  In more details, if $\lambda/2 < L_x$ the entire process takes place in the $H \neq 0$ region
- Consider $\varepsilon_\gamma \neq m_a$, so that $q_1 \geq m_a + 1/2L$, $q_2 \leq m_a - 1/2L$
  Poles coincide when $\varepsilon_\gamma = m_a$ ($p^* = 0$)
  Minimum distance between poles must satisfy: $\min(q_1 - q_2) = 1/L$
- We argue the formula

$$P_{\gamma\to a} \approx G^2 H^2 \frac{\sin^2(q_x L_x/2)}{q_x^2} \frac{\epsilon_\gamma}{\frac{1}{L_x} + \sqrt{\epsilon_\gamma^2 - m_a^2}}$$

to be used when $\varepsilon_\gamma \approx m_a$ to avoid unphysical divergences

Axion-Like particles

$$\mathcal{L}_I = \frac{1}{M} a F_{\mu\nu} \tilde{F}^{\mu\nu}$$

$$\tilde{F}^{\mu\nu} = \frac{1}{2} \epsilon^{\mu\nu\rho\sigma} F_{\rho\sigma}$$

$$\Box a = \frac{1}{M} \vec{H}^{ext} \cdot \frac{\partial}{\partial t} \vec{A} - m^2 a$$

Cfr. Poisson eq. in electricity:

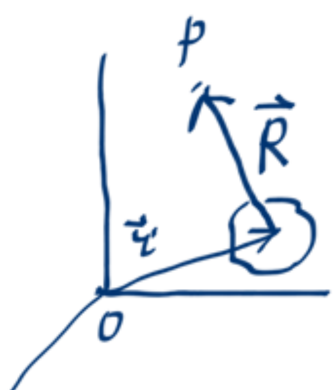

$$\Delta \phi + k^2 \phi = -4\pi \rho$$

$$\phi = \int \rho\left(\vec{r}', t - \frac{R}{c}\right) \frac{e^{ikR}}{R} dV'$$

$R \simeq r - \vec{r}' \cdot \vec{n}'$ $\quad \vec{k}' = k \vec{n}'$ $\quad r \gg r'$

Photon - Axion Conversion

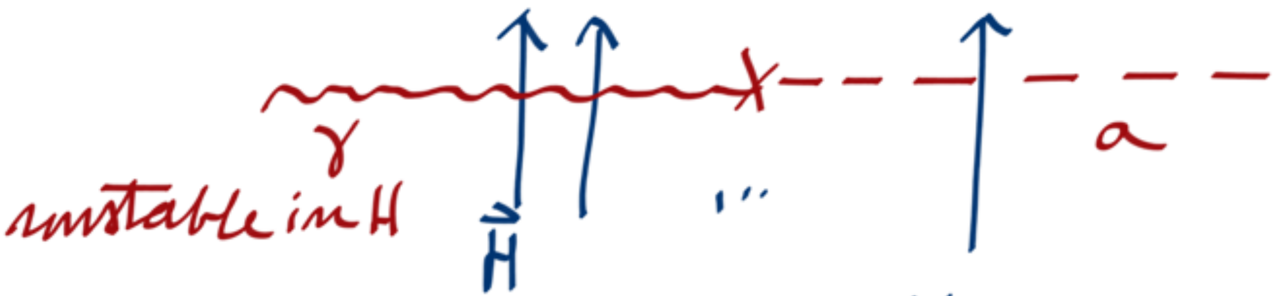

$$a = f\,\frac{e^{ikr}}{r}$$

$$\left|M_{\gamma \rightleftarrows a}\right|^2 = \frac{1}{4\pi^2}\left|\int e^{i\vec{q}\cdot\vec{r}}\,\vec{H}(\vec{r})\cdot\vec{E}(\vec{k}_\gamma,\lambda)\,dV\right|^2$$

Max when $\vec{k}_\gamma \perp \vec{H}$

Formula holds for $\mathcal{E}_\gamma = \mathcal{E}_a$

Notice $|\vec{k}_\gamma| \neq |\vec{k}_a|$ and $\vec{q} = \vec{k}_\gamma - \vec{k}_a$

Conversion Probability

In the $\perp$ plane H extends over long dist. wrt $1/q_y$ & $1/q_z$ - In the $\parallel$ direction we assume $L_x \lesssim 1/q_x$.

$$P_{\gamma \rightleftarrows a} = \frac{H^2}{M^2} \frac{\sin^2\left(\frac{q_x L_x}{2}\right)}{q_x^2} \left(\frac{E_\gamma}{|k_a|}\right)$$

$$q_x = \frac{m_a^2}{2E_\gamma}$$

$$|\vec{k}_a| = E_a^2 - m_a^2 = E_\gamma^2 - m_a^2 \sim E_\gamma \text{ as } E_\gamma \gg m_a$$

Dark photons

L.B. Okun, Sov. Phys.-JETP **56**, 502 (1982)
B. Holdom, Phys. Lett. B **166**, 196 (1986)

- Massive vectors of hidden $U(1)_h$

- Visible and hidden-sector photons Lagrangian:

$$\mathcal{L} = -\frac{1}{4}F^{\mu\nu}F_{\mu\nu} - \frac{1}{4}B^{\mu\nu}B_{\mu\nu} + eJ^{\mu}_{\rm em}A_{\mu} + e_{\rm h}J^{\mu}_{\rm h}B_{\mu} - \frac{1}{2}\mu^2 B^{\mu}B_{\mu}$$

$F^{\mu\nu}$ = field strength tensor for A^{μ}; $B^{\mu\nu}$ = field strength tensor for B^{μ} (paraphoton)

- **A** and **B** rotated into $\mathbf{B}_1$ and $\mathbf{B}_2$; mixing angle $\chi < 10^{-2}$

$\mathbf{B}_1$ and $\mathbf{B}_2$ acquire masses $m_1 = \mu\chi$, $m_2 = \mu$

- Photon field evolve as:

$$A(r) = \frac{1}{\chi^2+1}e^{-i(\epsilon_\gamma t - k_1 r)}\left[A(1+\chi^2 e^{-iqr}) + \chi B(e^{-iqr}-1)\right]$$

$$k_1 \approx \varepsilon_\gamma$$

$$k_2 \approx \sqrt{\varepsilon_\gamma^2 - \mu^2}$$

$$q = k_1 - k_2$$

Dark photons

L.B. Okun, Sov. Phys.-JETP **56**, 502 (1982)
B. Holdom, Phys. Lett. B **166**, 196 (1986)

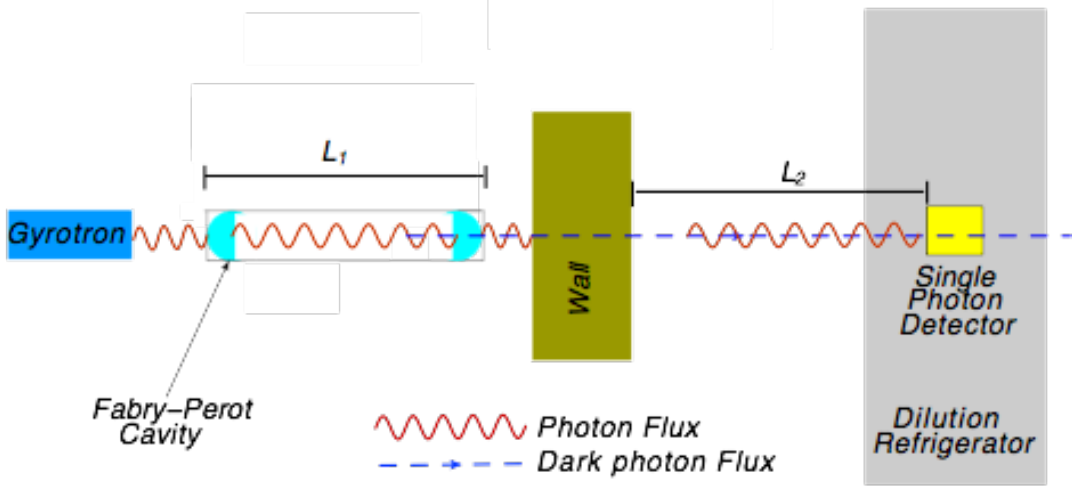

- Conversion probability: $P_{\gamma\to\gamma'}(r) = 4\chi^2 \sin^2\left(\frac{qr}{2}\right)$

$$P_{\gamma\to\gamma'\to\gamma} = P_{\gamma\to\gamma'}(L_1)P_{\gamma'\to\gamma}(L_2) = 16\chi^4\left[\sin\left(\frac{qL_1}{2}\right)\sin\left(\frac{qL_2}{2}\right)\right]^2$$

- Rate: $\frac{\mathrm{d}N_\gamma}{\mathrm{d}t} = \eta\,\Phi_\gamma\left[\frac{N_{\rm pass}+1}{2}\right]P_{\gamma\to\gamma'\to\gamma}$

Φ_γ = photon flux (s^{-1}), η = detector efficiency

Search for dark photons at STAX

L.M. Capparelli *et al.*, Phys. Dark Univ. **12**, 37 (2016)

- Exclusion limits STAX may achieve in case of null result

- **STAX** limits compared to
  - **ALPS LSW** results
    Phys. Lett. B **689**, 149 (2010)
  - **CROWS** results
    Phys. Rev. D **88**, 075014 (2013)
  - **Spring-8** results
    Phys. Lett. B **722**, 301 (2013)
  - **XENON10** results
    Phys. Lett. B **689**, 149 (2010)
  - Constraints on dark photons from measurements of the **CMB**
    Astrophys. J. **473**, 576 (1996)
  - Searches for modifications of **Coulomb's Law**
    Phys. Rev. Lett. **61**, 2285 (1988)